Science
AAAS

Band Formation from Coupled Quantum Dots Formed by a Nanoporous Network on a Copper Surface

Jorge Lobo-Checa, *et al.*

Science **325**, 300 (2009);
DOI: 10.1126/science.1175141

The following resources related to this article are available online at www.sciencemag.org (this information is current as of July 17, 2009):

Updated information and services, including high-resolution figures, can be found in the online version of this article at:
http://www.sciencemag.org/cgi/content/full/325/5938/300

Supporting Online Material can be found at:
http://www.sciencemag.org/cgi/content/full/325/5938/300/DC1

This article **cites 27 articles**, 5 of which can be accessed for free:
http://www.sciencemag.org/cgi/content/full/325/5938/300#otherarticles

This article appears in the following **subject collections**:
Physics
http://www.sciencemag.org/cgi/collection/physics

Information about obtaining **reprints** of this article or about obtaining **permission to reproduce this article** in whole or in part can be found at:
http://www.sciencemag.org/about/permissions.dtl

Science (print ISSN 0036-8075; online ISSN 1095-9203) is published weekly, except the last week in December, by the American Association for the Advancement of Science, 1200 New York Avenue NW, Washington, DC 20005. Copyright 2009 by the American Association for the Advancement of Science; all rights reserved. The title *Science* is a registered trademark of AAAS.

shown in Fig. 3. The onset of the decrease of $g^{(n)}(\tau = 0)$ coincides with the beginning of the LP blue shift and the onset of a nonlinear increase in the input-output curve. This shows that the system leaves the strong coupling regime and starts to lase. At high excitation powers, well-defined lasing at the bare cavity mode builds up as expected (Fig. 2). It is obvious that the thresholds, where the $g^{(n)}(\tau = 0)$ begin to decrease toward a value of 1, do not occur at the same excitation density. This shift can be explained in terms of the low photon numbers inside the cavity at the lasing threshold. Stimulated emission sets in at a mean photon number p of the order of unity inside the mode of interest, but in the threshold region, there is still a superposition of thermal and stimulated emission present. Because of the stronger photon number fluctuations in chaotic fields, their contribution to n-photon combinations will still be substantial, whereas p is smaller than n.

Our results verify that, under nonresonant excitation, the ground state of a semiconductor microcavity in the strong coupling regime is a single-mode thermal light source and shows particularly pronounced bunching effects, even in higher orders. In terms of applications, our findings are promising for applications in quantum-optical coherence tomography or ghost imaging optics and allow for thermal light imaging, offering high temporal resolution and massively improved sensitivity for n-photon processes as compared with coherent light. From a more fundamental point of view, the demonstrated experimental technique is a versatile tool for studying quantum fluctuations and phase transitions and might especially provide further insight into the intensely debated physics of polariton lasers and the spontaneous phase transition toward polariton Bose-Einstein condensates (*17*).

References and Notes

1. R. Hanbury Brown, R. Q. Twiss, *Nature* **177**, 27 (1956).
2. F. T. Arecchi, E. Gatti, A. Sona, *Phys. Lett.* **20**, 27 (1966).
3. G. Baym, *Act. Phys. Pol. B* **29**, 1839 (1998).
4. S. Fölling *et al.*, *Nature* **434**, 481 (2005).
5. U. Fano, *Am. J. Phys.* **29**, 539 (1961).
6. G. Scarcelli, V. Berardi, Y. Shih, *Phys. Rev. Lett.* **96**, 063602 (2006).
7. U. M. Titulaer, R. J. Glauber, *Phys. Rev.* **140**, B676 (1965).
8. G. S. Agarwal, *Phys. Rev. A* **1**, 1445 (1970).
9. B. L. Morgan, L. Mandel, *Phys. Rev. Lett.* **16**, 1012 (1966).
10. S. M. Ulrich *et al.*, *Phys. Rev. Lett.* **98**, 043906 (2007).
11. P. Michler *et al.*, *Science* **290**, 2282 (2000).
12. J. Kasprzak *et al.*, *Phys. Rev. Lett.* **100**, 067402 (2008).
13. D. M. McAlister, M. G. Raymer, *Phys. Rev. A* **55**, R1609 (1997).
14. V. Savona, F. Tassone, C. Piermarocchi, A. Quattropani, P. Schwendimann, *Phys. Rev. B* **53**, 13051 (1996).
15. Materials and methods are available as supporting material on *Science* Online.
16. J. R. Jensen, P. Borri, W. Langbein, J. M. Hvam, *Appl. Phys. Lett.* **76**, 3262 (2000).
17. P. Schwendimann, A. Quattropani, *Phys. Rev. B* **77**, 085317 (2008).

18. We thank C. B. Sørensen for growing the wafer and I. Akimov for discussions. This work was supported by the Deutsche Forschungsgemeinschaft research group "Quantum optics in semiconductor nanostructures." A patent application for the optical setup presented here is currently being filed.

Supporting Online Material

www.sciencemag.org/cgi/content/full/325/5938/297/DC1
Materials and Methods
SOM Text
References

3 April 2009; accepted 8 June 2009
10.1126/science.1174488

Band Formation from Coupled Quantum Dots Formed by a Nanoporous Network on a Copper Surface

Jorge Lobo-Checa,[1]*†‡ Manfred Matena,[1]† Kathrin Müller,[2] Jan Hugo Dil,[3,4] Fabian Meier,[3,4] Lutz H. Gade,[5] Thomas A. Jung,[2]‡ Meike Stöhr[1]‡

The properties of crystalline solids can to a large extent be derived from the scale and dimensionality of periodic arrays of coupled quantum systems such as atoms and molecules. Periodic quantum confinement in two dimensions has been elusive on surfaces, mainly because of the challenge to produce regular nanopatterned structures that can trap electronic states. We report that the two-dimensional free electron gas of the Cu(111) surface state can be trapped within the pores of an organic nanoporous network, which can be regarded as a regular array of quantum dots. Moreover, a shallow dispersive electronic band structure is formed, which is indicative of electronic coupling between neighboring pore states.

The electronic and optical properties of crystalline solids exhibit properties that derive to a large extent from the periodic arrangement and interactions of their component quantum systems, such as atoms or molecules. Extending the principle of such periodic coupling beyond the molecular regime has given rise to metamaterials, which are composed of regularly repeated units (*1*), in most cases, nanoparticles (*2*, *3*). Quantum effects that arise from confinement of electronic states have been extensively studied for surface states of noble metals, which are characterized by a quasi–two-dimensional (2D) electron gas. These may be visualized by scanning tunneling microscopy (STM) as standing wave patterns arising from scattering at steps and defects (*4*, *5*) or at large organic molecules (*6*). Examples of such surface state confinement comprise thin films (*7*), artificial nanoscale structures (*8*, *9*), vacancy and ad-atom islands (*10*, *11*), self-assembled 1D chains (*12*, *13*), vicinal surfaces (*14*–*16*), and quantum dots (*2*, *17*).

In spite of these previous examples, periodic quantum confinement in 2D at surfaces has always been elusive, mainly because of the difficulties encountered in the production of strictly regular nanopatterned structures that can trap electronic states. However, we note that Collier *et al.* observed coupling phenomena between quantum dots at a solid-liquid interface, namely between colloidal particles arranged in a Langmuir monolayer (*17*).

Periodic confinement in 2D is expected to induce regularly distributed discrete energy levels that could be experimentally observed through the appearance of nondispersive subbands, as previously reported for thin films (*7*) or 1D systems (*13*, *15*, *16*). The size of the confining entities embedded within the 2D periodic nanostructures should be larger than or comparable to a critical length of ~2 nm, as experimentally observed for 1D structures (*15*). The design of such structures is more readily achieved by using molecules as building blocks rather than atomic units, given the fundamental dimensions of these arrays. Potential candidates for molecular systems that might exhibit this zero-dimensional (0D) periodic electronic confinement are porous molecular surface networks. Their production is based on molecular self-assembly, which makes use of concepts established in supramolecular chemistry and has the advantage that identical parts are produced at once. This is in contrast, for instance, to assembly based on atom-by-atom positioning techniques (*8*, *9*). Self-assembled nanoporous networks have been obtained by using either hydrogen bonding motifs (*18*) or metal-complexation (*19*) on metal surfaces. Within the pores of these molecular nanoporous networks, electronic confinement is to be expected (*20*).

We report on the interplay of the surface state electrons of Cu(111) with a supramolecular porous network adsorbed on the Cu surface that leads to the formation of a 2D electronic band structure through the coupling of confined elec-

---

[1] Department of Physics, University of Basel, CH-4056 Basel, Switzerland. [2] Laboratory for Micro- and Nanotechnology, Paul Scherrer Institute, CH-5232 Villigen PSI, Switzerland. [3] Physik-Institut, Universität Zürich, Winterthurerstrasse 190, CH-8057 Zürich, Switzerland. [4] Swiss Light Source, Paul Scherrer Institute, CH-5232 Villigen, Switzerland. [5] Anorganisch-Chemisches Institut, Universität Heidelberg, Im Neuenheimer Feld 270, 69120 Heidelberg, Germany.

*Present address: Centre d'Investigaciò en Nanociència i Nanotecnologia (CIN2), 08193 Bellaterra (Barcelona), Spain.
†These authors contributed equally to this work.
‡To whom correspondence should be addressed. E-mail: jorge.lobo@cin2.es (J.L.-C.); thomas.jung@psi.ch (T.A.J.); meike.stoehr@unibas.ch (M.S.)

tronic states. We chose a perylene derivative, 4,9-diaminoperylene-quinone-3,10-diimine (DPDI), as the organic building block (Fig. 1A), which forms a highly ordered network on Cu(111) upon thermal dehydrogenation (*21*). By choice of the appropriate molecular coverage before annealing (*22*) a highly stable hexagonal p(10x10) organic superstructure is generated (Fig. 1B) (*21*, *23*). Each pore of the network confines the surface state of the Cu substrate in what can be described as a 0D quantum dot. Because of the imperfect confinement observed for all 0D cases studied so far on surfaces (*8*–*12*), coupling of quantum dots with their neighbors results in shallow dispersive electronic bands. Our results may suggest possible modifications of these artificially created electronic structures, such as changes to the dimensions of the molecular network periodicities together with the appropriate choice of the substrate.

We used scanning tunneling spectroscopy (STS) to probe the local (electronic) density of states (LDOS) (*24*). Spectra recorded inside a pore display a peak at –0.22 V that is not seen on the bare metal (Fig. 2A). Given the previous observations of discrete states in 2D nanostructures (*8*–*11*), we assign this peak to the confinement of the surface state electrons inside the pore. The confinement of this discrete state is demonstrated by recording simultaneously topography (Fig. 2B) and *dI*/*dV* (differential conductance) signal (Fig. 2C) at the peak energy, the latter showing in first order the local distribution of this state. Because each pore features a confined state, it can be considered as a single quantum dot that confines electrons in all three directions. The inherent periodicity of the molecular network generates a regular "quantum dot array" (Fig. 2C).

The width of the STS peak in Fig. 2A suggests imperfect confinement, which has been previously observed for isolated 2D nanocavities (*8*–*11*) as well as for 1D confinement (*12*). Such cases can be explained by lossy scattering at the confining boundary; inelastic electron-electron and electron-phonon scattering in small nanocavities are thought to be less important (*11*). Likewise, for our 2D periodic dehydro-DPDI network, which is commensurate with the Cu(111) substrate, the confined electronic states are expected to "leak" into neighboring pores. This leakage would electronically couple quantum wells of neighboring pores, and this coupling should be visible in the electronic structure of the system.

The electronic structure of our quantum dot array was investigated with angle-resolved photoemission spectroscopy (ARPES). This laterally averaging surface-sensitive technique determines the binding energy of the occupied states of the system as a function of the electron momentum. In Fig. 3A, ARPES normal emission spectra recorded at room temperature (RT) are shown for the clean Cu substrate and for the Cu substrate covered by different amounts of the dehydro-DPDI network. For the extreme cases (the clean Cu substrate and the highest molecular coverage), the spectra display a single component line shape, whereas all the other spectra exhibit a double-peak line shape. A detailed analysis of the spectra (fitted by using two Lorentzian components together with a constant background and multiplied by a Fermi-Dirac distribution) shows that the double peak consists of the components observed for the extreme cases, whereas only their relative intensities vary depending on the network coverage (Fig. 3B). The component marked red is attributed to the clean surface state and maintains its binding energy and width

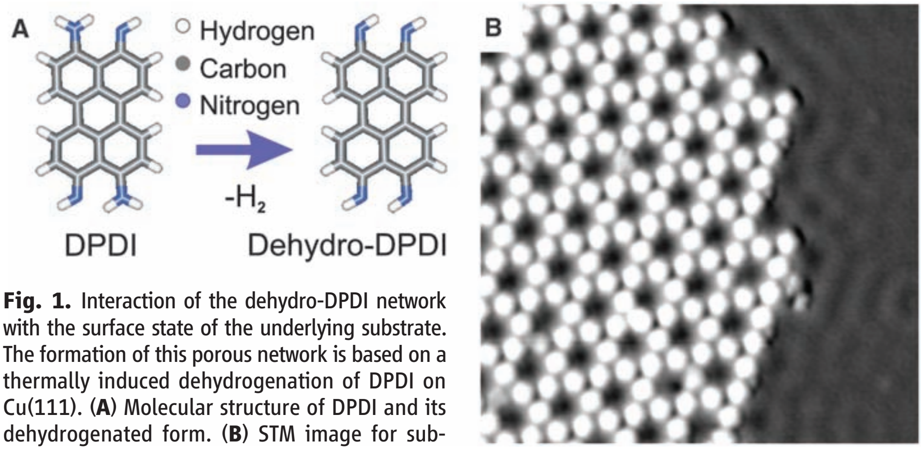

Fig. 1. Interaction of the dehydro-DPDI network with the surface state of the underlying substrate. The formation of this porous network is based on a thermally induced dehydrogenation of DPDI on Cu(111). (**A**) Molecular structure of DPDI and its dehydrogenated form. (**B**) STM image for submonolayer coverage of DPDI deposited on Cu(111) after thermal annealing at 500 K. Dehydro-DPDI acts as both hydrogen-bond donor and acceptor to produce a very stable self-assembled porous network (image size: 29 nm by 29 nm, –0.1 V, 50 pA) (*21*). The network periodicity is 2.55 nm with a pore diameter of ~1.6 nm. Standing wave patterns in the Cu surface state arise from the scattering of the delocalized electronic states at the border of the adsorbate adlayer. This can be observed at low tunneling bias (*4*–*6*).

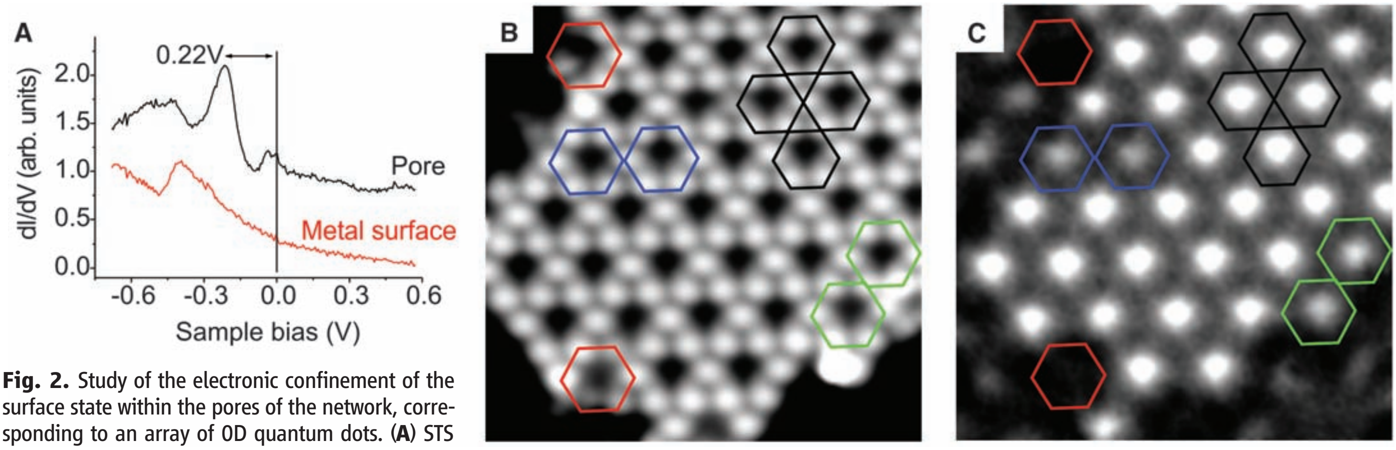

Fig. 2. Study of the electronic confinement of the surface state within the pores of the network, corresponding to an array of 0D quantum dots. (**A**) STS spectra obtained at 5 K on the clean Cu surface (red) and inside a pore of the dehydro-DPDI network (black). The latter spectrum exhibits a maximum at –0.22 V, which is attributed to a confined surface state (lock-in: V_{rms} = 6 mV, f = 513 Hz, initial tip parameters: –0.8 V/80 pA). (**B**) STM image of the porous network (13.6 nm by 13.6 nm, –0.20 V, 70 pA) and (**C**) simultaneously recorded *dI*/*dV* map at 5 K (lock-in: V_{rms} = 8 mV, f = 513 Hz). A confined electronic state is observed inside the molecular pores. The black hexagons highlight the molecular positions. Defective pores severely affect the confined state (red hexagons), although not every defect annihilates the confined state (green hexagons). In some cases, the confined state is affected although topography does not indicate any defects (blue hexagons). These observations could be explained by irregularities of the substrate within the pore (e.g., trapped Cu ad-atoms or holes).

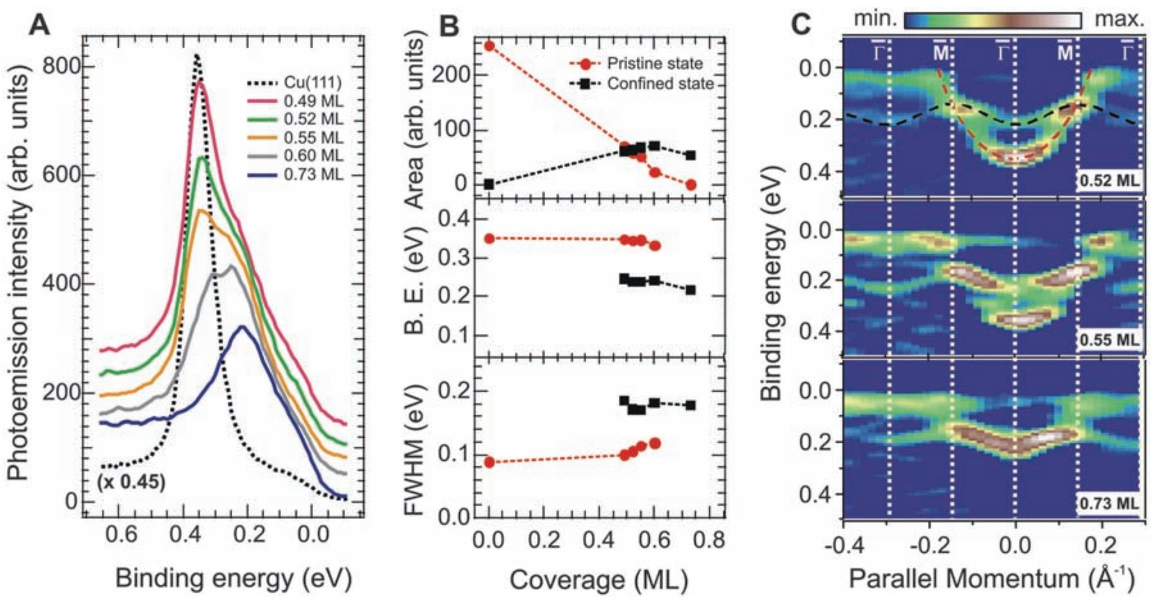

Fig. 3. Band dispersion resulting from the periodic influence of the porous network on the surface state studied with ARPES for different molecular coverages. (**A**) Normal emission spectra at RT showing the emerging confined state, which progressively replaces the original Cu(111) surface state (scaled, black dotted line) with increasing molecular coverage. (**B**) Peak area, binding energy (B.E.), and full width at half maximum (FWHM) resulting from the analysis of the pristine and the confined states presented in (A). (**C**) Energy dispersion curves (EDCs) of the pristine state (red dashed line) and the confined state (black dashed line) measured along the $\overline{\Gamma M}$ high symmetry direction and visualized as the second derivative of the photoemission intensity for three different coverages. The second derivative was used to enhance features of the EDC. Both EDCs at 0.52 ML and 0.73 ML were acquired at RT, whereas 60 K was the acquisition temperature for 0.55 ML. The vertical white dotted lines refer to the new symmetry points induced by the molecular network. The red and black dashed lines on the top graph indicate the averaged positions of the maxima of both Lorentzian components fitted for all EDCs.

throughout the molecular coverage range, but its intensity decreases as the molecular network coverage increases. It will be referred to below as the pristine state. The component marked black, however, is related to the influence of the molecular network and increases with increasing coverage. In analogy to the pristine case, it has a constant width and a constant binding energy. Its value of 0.23 ± 0.03 (experimental error) eV is in very good agreement with the STS spectrum shown in Fig. 2A. Because its binding energy and peak width are independent of the surface coverage, its origin can be attributed to a single pore with its surrounding molecular border, whereas the overall island size shows no influence. This component will be referred to below as the confined state.

Isolated nanocavities exhibit discrete electronic states, but the periodic influence of the porous network on the 2D free electron gas of the surface state, along with the imperfection of its confinement, is expected to induce an electronic band in analogy to the band structure of a solid created by the periodic potential of its atoms. The existence of such cooperative behavior can be investigated by studying with ARPES the electronic structure of both the pristine Cu(111) surface state and the confined state as a function of the surface parallel momentum. The ARPES data displayed in Fig. 3C exhibit for both states dispersive bands. One band (highlighted in red) follows the characteristic parabolic dispersion of the Cu surface state (*25*), whereas the second band (highlighted in black) is related to the periodic potential of the porous network. This interpretation is supported by the periodic continuation of the band within Brillouin zones of higher order that possess the same periodicity as the molecular network (10 times smaller than the substrate). This periodicity is indicated by white lines in Fig. 3C, which are separated by $|k_{\text{parallel}}| = 0.142$ Å^{-1}. Furthermore, weak photoemission intensity very near the Fermi energy and around the $\overline{M}$ symmetry points can also be observed in Fig. 3C, especially for the case of 0.55 monolayer (ML), which was acquired at 60 K. In analogy to the 1D case (*15*, *16*), we attribute this intensity to the existence of the second subband, which has its lowest binding energy at ~60 meV. This value matches perfectly the onset of the second peak observed in the pore STS spectrum of Fig. 2A. Thus, the energy gap between the subbands originating from the confined network is ~90 meV.

The rather shallow dispersing band (bandwidth of ~80 meV) is an indication of the strong confinement of the surface state inside the pores. Further evidence for our interpretation stems from both STS measurements performed on top of dehydro-DPDI molecules and photoemission spectra acquired on a sample fully covered by a close-packed structure of dehydro-DPDI (*21*, *23*). For this nonporous organic network of the same building block, no evidence of the surface state was found, which additionally corroborates the strong confinement of the surface state within the pores. In analogy to the textbook case of electronic states in the solid crystal (*26*), it is the balance of confinement and coupling between neighboring quantum systems that leads to the formation of an electronic band. In our case, the final electronic structure results from the dimensions of the porous network together with the interaction of the molecular backbone with the 2D surface electronic state.

Our results provide conclusive experimental evidence of periodic 2D confinement by a porous molecular network, which can be regarded as a regular array of 0D quantum dots. A notable consequence of such periodic influence on the otherwise free electron–like surface state is the formation of an artificial electronic band structure. The established and prospective possibilities to control the structures of porous networks, together with the characteristic degree of coupling between ad-molecules and the surface state, will allow the fabrication of related systems with different band structures, resulting in 2D electronic metamaterials in analogy to the well-established optical metamaterials (*27*, *28*). These findings may also provide new insight into the behavior of molecular guests within porous host networks on surfaces (*29*, *30*), and the expected influence of the guests on the electronic band structure may even induce long-range effects in their host-guest behavior (*31*). Moreover, the resulting electronic bands may play a decisive role in the stabilization of the porous networks themselves.

References and Notes

1. R. M. Walser, *Proc. SPIE* **4467**, 1 (2001).
2. F. X. Redl, K.-S. Cho, C. B. Murray, S. O'Brien, *Nature* **423**, 968 (2003).
3. A. L. Rogach, *Angew. Chem. Int. Ed.* **43**, 148 (2004).
4. M. F. Crommie, C. P. Lutz, D. M. Eigler, *Nature* **363**, 524 (1993).
5. Y. Hasegawa, P. Avouris, *Phys. Rev. Lett.* **71**, 1071 (1993).
6. L. Gross *et al.*, *Phys. Rev. Lett.* **93**, 056103 (2004).
7. T.-C. Chiang, *Surf. Sci. Rep.* **39**, 181 (2000).
8. M. F. Crommie, C. P. Lutz, D. M. Eigler, *Science* **262**, 218 (1993).
9. J. Kliewer, R. Berndt, S. Crampin, *New J. Phys.* **3**, 22 (2001).
10. J. Li, W.-D. Schneider, R. Berndt, S. Crampin, *Phys. Rev. Lett.* **80**, 3332 (1998).
11. H. Jensen, J. Kröger, R. Berndt, S. Crampin, *Phys. Rev. B* **71**, 155417 (2005).
12. Y. Pennec *et al.*, *Nat. Nanotechnol.* **2**, 99 (2007).
13. U. Bischler, E. Bertel, *Phys. Rev. Lett.* **71**, 2296 (1993).
14. O. Sánchez *et al.*, *Phys. Rev. B* **52**, 7894 (1995).
15. A. Mugarza, J. E. Ortega, *J. Phys. Condens. Matter* **15**, S3281 (2003).

16. J. Lobo *et al.*, *Phys. Rev. Lett.* **93**, 137602 (2004).
17. C. P. Collier, R. J. Saykally, J. J. Shiang, S. E. Henrichs, J. R. Heath, *Science* **277**, 1978 (1997).
18. J. A. Theobald, N. S. Oxtoby, M. A. Phillips, N. R. Champness, P. H. Beton, *Nature* **424**, 1029 (2003).
19. U. Schlickum *et al.*, *Nano Lett.* **7**, 3813 (2007).
20. N. Herron, *J. Inclusion Phenom. Macrocyclic Chem.* **21**, 283 (1995).
21. M. Stöhr *et al.*, *Angew. Chem. Int. Ed.* **44**, 7394 (2005).
22. One monolayer (ML) refers to a full coverage of a close-packed assembly of DPDI. A full surface coverage of the porous network occurs at a coverage of ~0.70 ML[21].
23. Materials and methods are available as supporting material on *Science* Online.
24. R. Wiesendanger, Ed., *Scanning Probe Microscopy and Spectroscopy: Methods and Applications* (Cambridge Univ. Press, Cambridge, 1994).
25. F. Reinert, G. Nicolay, S. Schmidt, D. Ehm, S. Hüfner, *Phys. Rev. B* **63**, 115415 (2001).
26. N. Ashcroft, D. Mermin, Eds., *Solid State Physics* (Saunders College, New York, 1976).
27. R. A. Shelby, D. R. Smith, S. Schultz, *Science* **292**, 77 (2001).
28. D. R. Smith, J. B. Pendry, M. C. K. Wiltshire, *Science* **305**, 788 (2004).
29. M. Stöhr, M. Wahl, H. Spillmann, L. H. Gade, T. A. Jung, *Small* **3**, 1336 (2007).
30. H. Dil *et al.*, *Science* **319**, 1824 (2008).
31. A. Kiebele *et al.*, *ChemPhysChem* **7**, 1462 (2006).
32. We thank H.-J. Güntherodt for continuous support; J. Osterwalder and T. Greber for fruitful discussions and providing access to the ARPES experimental station, hosted at the Surface and Interface Spectroscopy beamline of the Swiss Light Source, Paul Scherrer Institut, Villigen, Switzerland; and Nanonis for fruitful collaboration on the STM/STS data acquisition system. Supported by the Swiss National Science Foundation, the National Center of Competence in Research "Nanoscale Science," the European Union through the Marie Curie Research Training Network PRAIRIES, the Wolfermann-Nägeli-Stiftung, the Bundesministerium für Bildung und Forschung (BMBF) Cluster "Forum Organic Electronics" (Heidelberg), and the Swiss Federal Commission for Technology and Innovation (CTI).

Supporting Online Material
www.sciencemag.org/cgi/content/full/325/5938/300/DC1
Materials and Methods
SOM Text
Figs. S1 to S7
References

20 April 2009; accepted 4 June 2009
10.1126/science.1175141

CH Stretching Excitation in the Early Barrier F + CHD_3 Reaction Inhibits CH Bond Cleavage

Weiqing Zhang,[1,2] Hiroshi Kawamata,[1] Kopin Liu[1]*

Most studies of the impact of vibrational excitation on molecular reactivity have focused on reactions with a late barrier (that is, a transition state resembling the products). For an early barrier reaction, conventional wisdom predicts that a reactant's vibration should not couple efficiently to the reaction coordinate and thus should have little impact on the outcome. We report here an in-depth experimental study of the reactivity effects exerted by reactant C-H stretching excitation in a prototypical early-barrier reaction, F + CHD_3. Rather counterintuitively, we find that the vibration hinders the overall reaction rate, inhibits scission of the excited bond itself (favoring the DF + CHD_2 product channel), and influences the coproduct vibrational distribution despite being conserved in the CHD_2 product. The results highlight substantial gaps in our predictive framework for state-selective polyatomic reactivity.

Not all forms of energy are equally effective in driving chemical reactions. Several decades of theory and experiment in reaction dynamics culminated in the Polanyi rules (*1*, *2*), which predict that, in reactions of an atom with a diatomic molecule, reactant vibration and translation have different impacts on the rate. When the barrier is located late along the reaction coordinate (i.e., the transition state resembles products more than reactants), the vibration is considered the more effective driver; the reverse is true for reactions with early barriers (*3*). A similar line of thought underlies efforts directed toward mode-selective chemistry in reactions involving polyatomics. It is now well documented, both in the gas phase (*4*–*14*) and at surfaces (*15*–*17*), that excitation of different vibrational motions of a polyatomic reactant can exert a profound influence on chemical reactivity. An intuitively appealing picture emerging from these studies is that exciting a vibrational mode with large displacements along a particular reaction coordinate can preferentially promote the system over the barrier of that pathway, leading to mode-dependent reactivity. The atomic-level mechanism governing this selectivity remains elusive, however.

Previous mode-specific studies have focused on reactions with a late barrier, which seems sensible from the perspective of an extended Polanyi rule framework (*10*). In an early-barrier reaction, reactant vibrations are commonly believed not to couple efficiently to the reaction coordinate. Contrary to this current perception, we report on an experiment that poses serious challenges to our fundamental understanding, even in a qualitative sense, of the vibrational effect on reactivity.

The reaction of F + CHD_3 is highly exothermic, enthalpy of reaction ~ –31 kcal/mol, and, based on Hammond's postulate (*1*), can be regarded as a prototypical early-barrier reaction. Consistent with this characterization, a recent, accurate ab initio calculation of the global potential energy surface indicates a reactant-like transition state structure, Fig. 1, left (*18*). Experimentally, both the thermal rate constant data (*19*) and the crossed-beam scattering results (*20*) suggest a small (<0.4 kcal/mol) barrier to reaction. Previously, comprehensive crossed-beam investigations of the ground state reaction have revealed roughly equal branching to two isotopic product channels, HF + CD_3 and DF + CHD_2 (*20*); numerous rovibrational product states were populated in each channel (*21*–*23*). We explored the impact on this reaction of one quantum excitation of the C-H stretching vibration ($v_1 = 1$) of CHD_3.

On the basis of the extended Polanyi rule framework described above, we considered several qualitative predictions of the outcome. Given the early barrier, would the vibrational excitation increase the rate relative to the ground state reaction at fixed translational energy? The previously observed equal branching to HF and DF products in the ground state reaction was a clear sign of nonstatistical behavior (*20*). Would initial deposition of vibration energy directly into the C–H bond facilitate its breakage to form HF + CD_3 preferentially? Lastly, the localized nature of the C-H stretch mode suggests that this bond should act as a spectator if the F atom were to attack the D atoms. In keeping with this spectator model (*5*), would the local CH stretching motion retain its vibrational character during the reaction, favoring the CHD_2 product with one-quantum excitation of the CH stretching mode ($v_1 = 1$) over ground state CHD_2 ($v = 0$)?

To seek answers to these questions, we performed a crossed-beam scattering experiment under single-collision conditions. The experimental apparatus consisted of two rotatable pulsed molecular beams and a fixed detector assembly housed in a vacuum chamber (*23*, *24*). The F atom beam was generated by a pulsed high-voltage discharge of 5% F_2 seeded in a pulsed supersonic expansion of Ne at 6 atm. The CHD_3 beam was also produced by pulsed supersonic expansion of 35% CHD_3 seeded in He at 6 atm. Both beams were collimated by double skimmers and crossed in a differentially pumped scattering chamber; collision energy (E_c) was tuned by varying the intersection angle of the two molecular beams. A pulsed laser operating near 333 nm probed the nascent distribution of CHD_2

---

[1] Institute of Atomic and Molecular Sciences (IAMS), Academia Sinica, Post Office Box 23-166, Taipei, 10617 Taiwan. [2] State Key Laboratory of Molecular Reaction Dynamics, Dalian Institute of Chemical Physics, Chinese Academy of Sciences, Post Office Box 110 extension 11, Dalian 116023, People's Republic of China.

*To whom correspondence should be addressed. E-mail: kliu@po.iams.sinica.edu.tw